Oxidation of Metals, Vol. 14, No. 6, 1980

The Effects of Gaseous Pretreatment and Oxide Sintering on Oxidation of Ti–4.32 wt.%Nb Alloy

Richard L. Rawe* and Casimir J. Rosa†

Received June 28, 1979

Oxidation kinetics in either air or oxygen of prenitrided Ti–4.32 wt.%Nb alloy are investigated in the temperature range of 900–1200°C. Based on X-ray and electron microprobe analyses, thermogravimetric measurements, microhardness data, and sintering experiments, a quantitative oxidation model is developed to explain the gas–metal reactions. Temperature cycling experiments, in the temperature range of 900–1200°C and for a 12-hr duration, are performed in an attempt to reduce the oxidation rates of the alloy in air or oxygen. The oxidation resistance of nitrogen pretreated alloy is comparable to that in air and it is considerably higher than in oxygen alone.

KEY WORDS: oxidation; microhardness data; sintering experiments; electron microprobe analyses.

INTRODUCTION

Oxidation rates in air at 871 and 982°C, under 760 Torr, of Ti–Nb alloys containing 4.45 or 1.0 wt.%Nb were studied by Maynor *et al.*[1] They found that the alloys oxidize at a slower rate than pure Ti oxidized under identical conditions. Similar studies by Rosa[2] on Ti–4.32 wt.%Nb and Ti–4.37 wt.%Ta in either oxygen or air indicate that at elevated temperatures, 1000–1200°C, the alloys exhibit considerably higher oxidation resistance than Ti. The increase in oxidation resistance of the alloy may be attributed to the reduction in oxygen vacancy concentration in the protective oxide scale

*Department of Materials Science and Metallurgical Engineering, University of Cincinnati, Cincinnati, Ohio.

†Presently on academic leave at Max-Planck-Institut für Metallforschung, Institut für Werkstoffwissenschaften, Stuttgart, Bundesrepublik Deutschland.

0030-770X/80/1200-0549$03.00/0

and can be explained by the Wagner–Hauffe theory[3] of binary-alloy oxidation. According to the theory a decrease in the oxidation rate of a metal (Ti) forming an n-type conducting oxide (TiO_{2-x}) can be expected upon addition of a higher valence cation (Nb^{5+}) than the valence of the base–oxide cation (Ti^{4+}) if the introduced cation is uniformly soluble in the base oxide.

The amount of work done in the past on nitridation of Ti and its alloys has been considerably less extensive than on oxidation, but it has been known for a long time[4–6] that the nitridation rates of pure Ti in the temperature range of about 550–1000°C are much lower than its oxidation rates. McDonald and Wallwork[6] report that during nitridation each Ti–N phase is present within the composition and temperature ranges of its thermodynamic stability as given by their Ti–N equilibrium phase diagram.

Münster and Schlamp[7] investigated the oxidation of TiN in oxygen at 760 Torr in the temperature range 625–1075°C for times up to 6 hr and it is found that the oxidation rates of TiN are significantly lower than those of pure Ti.[8]

The present investigation is an attempt to further reduce the oxidation kinetics of the Ti–4.32 wt.%Nb alloy by means of two methods: (i) by oxidizing either in oxygen or air of prenitrided alloy, this method being referred to as nitrogen pretreatment; and (ii) by cycling of the oxidizing temperature of the alloy and oxidizing it in either oxygen or air for 4-hr periods; this method being here referred to as oxide sintering. Oxidation kinetics of the alloy without nitrogen pretreatment or oxide sintering are given as comparative references.

EXPERIMENTAL

Samples of approximately $1.5 \times 1.5 \times 0.2$ cm were cut from a cold-rolled sheet of Ti–4.32 wt.%Nb with the following impurity analyses (in wt.%): $Hf < 0.01$, Fe = 0.043, N = 0.011, O = 0.107, C = 0.018, and H = 0.0044. Thus obtained coupons were polished on 180 through 600 grit SiC papers and final polishing was performed with 6- and 1-μ diamond pastes. The surface area, A_0, of each sample was determined as the average of three micrometric measurements across the rectangular dimensions. To prevent abnormal grain growth during the nitridation and/or oxidation experiments all samples were vacuum annealed at 10^{-5} Torr for 2 hr at a temperature 50°C higher than the highest actual temperatures of the subsequently performed experiments.

The weight gain of the nitrided and/or oxidized samples was continuously monitored by a Cahn, RH, electrobalance in conjunction with a Leeds and Northrup, Speedomax X/L 680, dual-pen chart recorder. The sensitivity of the electrobalance is ~0.9 μg for samples with the approximate

total surface area of 5.46 cm^2 used in this investigation. The second pen was used to record the experiment temperature simultaneously with the weight gain. The temperature was monitored to within ±3°C of the present temperatures by a Pt–Pt/10%Rh thermocouple placed about 2 mm from the specimen surface. A Marshal 4045 current-proportional controller was used to adjust the preset temperature of the furnace, inside which a sample was suspended by a 0.005-cm diam. Pt wire. All metal–gas reactions were performed at a pressure of 755 ± 2 Torr.

The purity of either oxygen or nitrogen used was better than 99.99 wt.% and no attempt was made to further purify or dry the gases. Dry laboratory air was used for kinetic measurements in air.

After kinetic measurements in various gaseous environments, the specimens were first examined by X-ray diffraction methods to determine the composition of the outer (oxide) scale. Following this, the outermost scale was mechanically removed, whenever possible, from the sample and X-ray diffractometer scans were then taken from each of the underlying surfaces. By using a paper-thin SiC cutoff wheel the specimens were next quartered. One quarter from each sample was mounted in Cu-filled AB diallyl phthalate, an electrical conducting thermosetting mounting material. After mechanical polishing with SiC papers and with 6, 1, and 0.25 μ diamond pastes these samples were examined by electron microprobe for the concentration profiles of Ti, Nb, O, and N across the sample thickness. The samples were also examined metallographically and Vickers microhardness measurements were taken at various positions on the cross section of some of the specimens. The remaining quarters were used for a more detail X-ray diffractometric scans or X-ray powder analyses by using a 114.6 mm diameter Debye-Scherrer camera and Ni-filtered CuKα radiation.

Sintering experiments at a temperature 100°C higher than the oxidation temperature were performed on the Ti–4.32 wt.%Nb alloy samples in an attempt to recrystallize the formed oxide scale and thus to lower the subsequent oxidation rate.

RESULTS

Nitridation Kinetics

The weight gain Δm per the initial total area A_0 of Ti–4.32 wt.%Nb samples is plotted vs. the exposure time, t, to nitrogen at seven temperature levels in Fig. 1 and the corresponding parabolic plots of the nitridation kinetics in Fig. 2. The parabolic rate constants, k_p, applicable to the nitridation period from which they were calculated, as well as the time

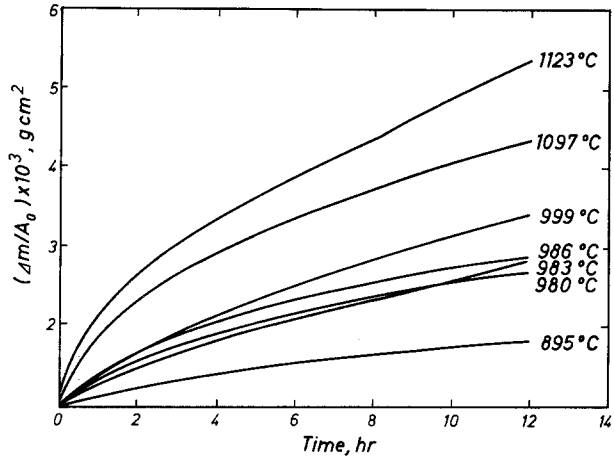

Fig. 1. Nitridation kinetics of Ti–4.32 wt.%Nb alloy at 755 Torr as a function of temperature.

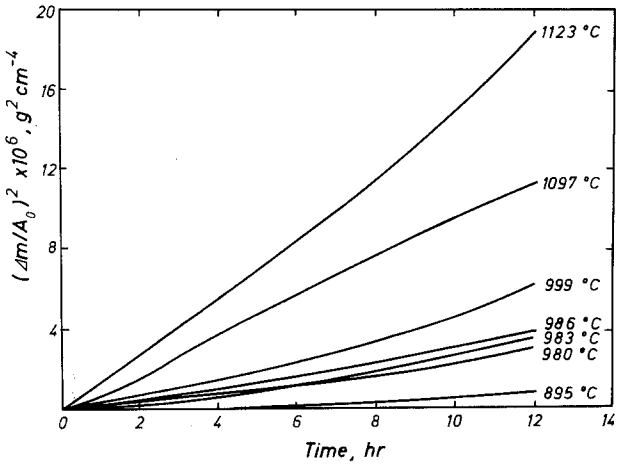

Fig. 2. Parabolic plots of nitridation kinetics of Ti–4.32 wt.%Nb alloy at 755 Torr as a function of temperature.

weighted average parabolic rate constants, $\overline{k_p}$, are listed in Table I. The latter constants are introduced to facilitate the comparison of the overall effect of the nitrogen pretreatment on subsequent oxidation and have been calculated from the equation:

$$\overline{k_p} = \sum_{i=1}^{n} (k_{p_i} t_i) \Big/ \sum_{i=1}^{n} t_i \qquad (1)$$

Table I. Parabolic Rate Constants (in $g^2 \cdot cm^{-4} \cdot sec^{-1}$) for Nitrogen Pretreatment of Ti–4.32 wt.%Nb Alloy

Temp., °C	Time, hr	k_p	$\overline{k_p}$
1123	0.5–8	4.0×10^{-10}	4.73×10^{-10}
	8–12	5.12×10^{-10}	
1097	0.5–12	2.65×10^{-10}	2.65×10^{-10}
999	0.5–6	9.8×10^{-11}	1.40×10^{-10}
	6–12	1.79×10^{-10}	
986	0.5–8	7.37×10^{-11}	9.33×10^{-11}
	8–12	1.30×10^{-10}	
983	0.5–6	1.41×10^{-11}	6.83×10^{-11}
	6–12	1.18×10^{-10}	
980	0.5–6	5.56×10^{-11}	5.56×10^{-11}
	6–12	8.33×10^{-11}	
895	0.5–6	5.13×10^{-12}	1.21×10^{-11}
	6–12	1.85×10^{-11}	

where k_{p_i} and the respective time t_i are obtained graphically from the slope of curves in Fig. 2. In spite of the clear tendency toward a linear nitridation rate after approximately 6–8 hr, we will use the average $\overline{k_p}$ as given by Eq. (1) to compare reaction rates with other gaseous treatments to be discussed later.

Oxidation After Nitridation

Oxidation of nitrogen pretreated Ti–4.32 wt.%Nb alloy results in approximately parabolic rates or, more commonly, in a sequence of parabolic rates as shown in Figs. 3 and 4 and summarized in Table II. For reference purposes, the oxidation kinetics of oxidized alloy without prior nitridation are also included. Clearly, the alloy oxidizes considerably faster in nonpretreated conditions at all of the investigated temperatures. The results also indicate that oxidation in laboratory air occurs at a slower rate than in pure oxygen and that this rate is, in turn, larger than that for specimens oxidized in air after prior nitridation.

An attempt has been made to correlate the parabolic rate constants k_p for the initial reaction periods (up to 6 hr) to temperature through an Arrhenius-type equation:

$$k_p = k_0 \exp(-Q/RT) \tag{2}$$

where Q is the activation energy (cal/mole), R is the ideal gas constant (1.98 cal/mole · °K) and T is the temperature in °K. Figure 5 is a semi-logarithmic plot of Eq. (2) and the activation energies obtained by the

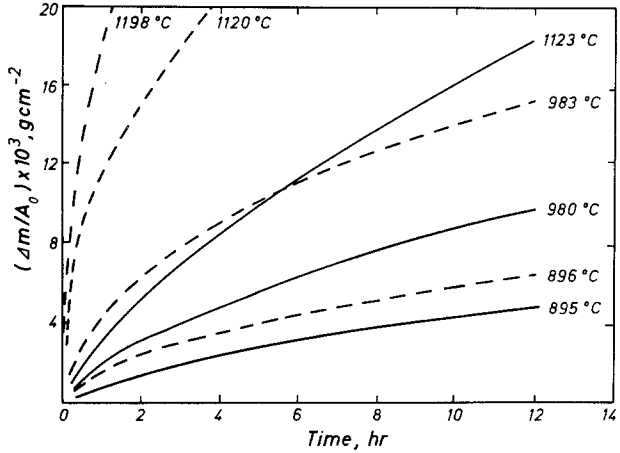

Fig. 3. Oxidation kinetics of Ti–4.32 wt.%Nb alloy in oxygen without nitrogen pretreatment (broken lines) and with nitrogen pretreatment (solid lines).

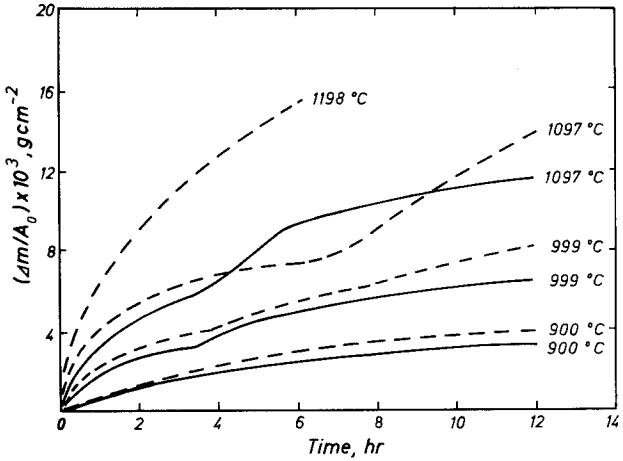

Fig. 4. Oxidation kinetics of Ti–4.32 wt.%Nb alloy in air without nitrogen pretreatment (broken lines) and with nitrogen pretreatment (solid lines).

least-squares method as well as the values of the preexponential term k_0 are listed in Table III.

Sintering

To investigate the oxide sintering effect on subsequent oxidation kinetics of the Ti–4.32 wt.%alloy, samples were first oxidized for 4 hr in

Table II. Parabolic Rate Constants (in $g^2 \cdot cm^{-4} \cdot sec^{-1}$) for Oxidation of Ti–4.32 wt.%Nb Alloy in Only Oxygen and in Oxygen After Nitrogen or Air Pretreatments

Temp., °C	Gas	Time, hr	k_p	$\bar{k}_p$
1198	Only O_2	0.5–3	9.65×10^{-8}	9.65×10^{-8}
1120	Only O_2	0.5–12	2.8×10^{-8}	2.8×10^{-8}
1123	O_2 after N_2	0.5–6	5.78×10^{-9}	7.96×10^{-9}
1123	O_2 after N_2	6–12	9.95×10^{-9}	
983	Only O_2	0.5–12	5.55×10^{-9}	5.55×10^{-9}
980	O_2 after N_2	0.5–7	1.72×10^{-9}	2.38×10^{-9}
980	O_2 after N_2	7–12	3.05×10^{-9}	
896	Only O_2	0.5–12	9.60×10^{-10}	9.60×10^{-9}
895	O_2 after N_2	0.5–6	3.94×10^{-10}	5.40×10^{-10}
895	O_2 after N_2	6–12	6.73×10^{-10}	
1198	Only air	0.5–6	1.10×10^{-8}	1.10×10^{-8}
1097	Only air	0.5–6	2.78×10^{-9}	5.40×10^{-9}
1097	Only air	6–12	7.81×10^{-9}	
1097	Air after N_2	0.5–4	3.17×10^{-9}	2.8×10^{-9}
1097	Air after N_2	4–6	5.56×10^{-9}	
1097	Air after N_2	6–12	1.85×10^{-9}	
999	Only air	0.5–4	7.95×10^{-10}	1.57×10^{-9}
999	Only air	4–8	1.74×10^{-9}	
999	Only air	8–12	2.08×10^{-9}	
999	Air after N_2	0.5–3.5	7.41×10^{-10}	4.11×10^{-10}
999	Air after N_2	3.5–12	2.94×10^{-10}	
900	Only air	0.5–12	3.21×10^{-10}	3.21×10^{-10}
900	Air after N_2	0.5–12	2.19×10^{-10}	2.19×10^{-10}

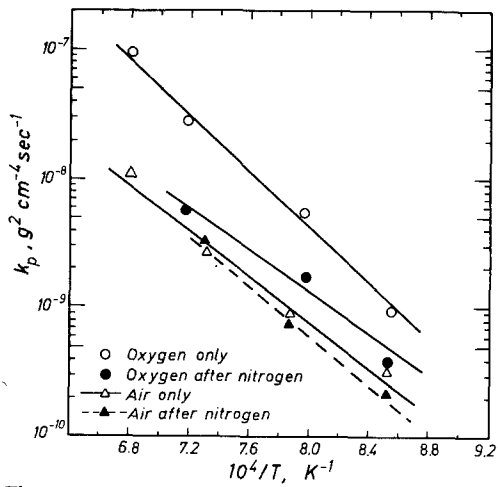

Fig. 5. Temperature dependence of the initial (up to 6 hr) parabolic rate constants for oxidation of Ti–4.32 wt.%Nb alloy.

Table III. Calculated Activation Energies for the Initial Oxidation Rates of Ti–4.32 wt.%Nb Alloy

Oxidation environment	Temp range, °K	Q, kcal/mole	k_0, g^2/cm^4 sec
Only oxygen	1169–1471	50.31	2.645
Only air	1173–1471	40.61	9.73×10^{-3}
Oxygen after nitridation	1168–1396	37.60	4.91×10^{-3}
Air after nitridation	1173–1370	43.11	2.21×10^{-2}

either pure oxygen or air. The reaction was then terminated by evacuating the system. The temperature was raised by 100°C above the initial reaction temperature and the gas was readmitted. Oxidation continued for the next 4 hr followed by lowering the temperature by 100°C in vacuum and, again, oxidizing the samples for an additional 4 hr. The oxidation kinetics prior to sintering, during sintering, and from the post-sintering period are given in Figs. 6–8. For comparison purposes included are also (dashed lines) the reaction kinetics for oxidation in pure oxygen or air in the absence of sintering. Table IV summarizes the calculated reaction rate constants. As can be seen, sintering of the oxide scale under the present experimental conditions does not reduce the subsequent oxidation rate at all of the investigated temperatures except, perhaps, for sintering in oxygen at 1200°C.

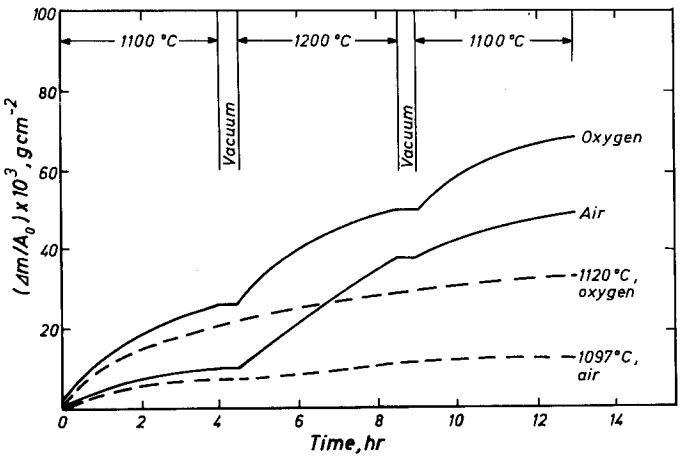

Fig. 6. Oxidation kinetics (solid lines) of Ti–4.32 wt.% Nb alloy at 1100°C and 755 Torr showing the effect of sintering at 1200°C.

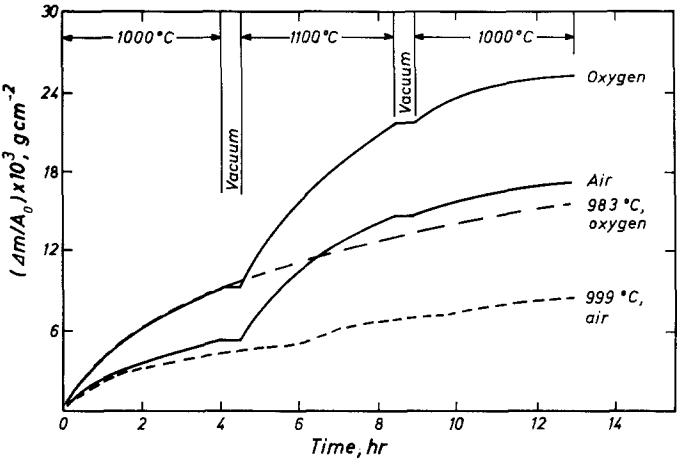

Fig. 7. Oxidation kinetics (solid lines) of Ti–4.32 wt.% Nb alloy at 1000°C and 755 Torr showing the effect of sintering at 1100°C.

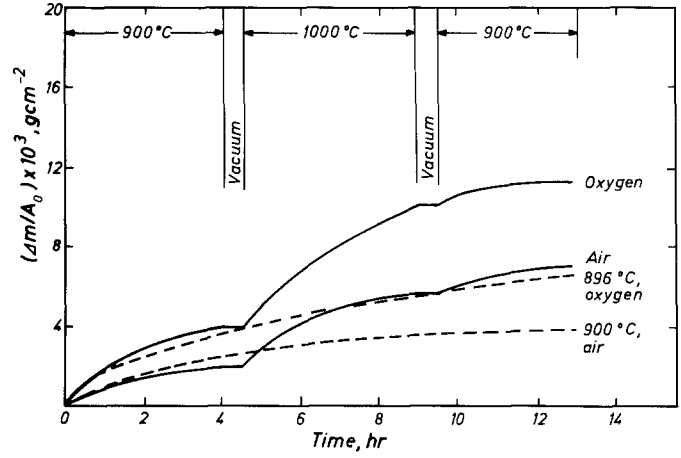

Fig. 8. Oxidation kinetics (solid lines) of Ti–4.32 wt.%Nb alloy at 900°C and 755 Torr showing the effect of sintering at 1000°C.

X-ray Diffraction

X-ray diffractometric scans from the outer scale surface formed on the Ti–4.32%Nb alloy reacted in oxygen-bearing environments (i.e., air, nitrogen pretreated plus oxidized in either air or oxygen, sintered in either air or oxygen) at any of the investigated temperatures revealed the presence

Table IV. Parabolic Rate Constants (in $g^2 \cdot cm^{-4} \cdot sec^{-1}$) for Each 4-hr Period of the Sintering Experiments on Ti–4.32 wt.%Nb Alloy

Sintering temp, °C; gas	$k_p \times 10^8$ 0.5–4 hr	4–8 hr	8–12 hr	$\bar{k}_p \times 10^8$ 0.5–12 hr
1200; oxygen	4.36	3.67	3.28	3.74
1200; air	0.521	9.03	0.870	3.60
1100; oxygen	0.569	2.92	1.14	1.58
1100; air	0.197	1.39	0.576	0.744
1000; oxygen	0.0986	0.590	0.0991	0.270
1000; air	0.0250	0.181	0.0889	0.101

of TiO_2 on all samples. This was confirmed by X-ray powder patterns obtained from the mechanically removed and ground outer scale of several specimens. X-ray diffractometric scans taken from the inner scale, beneath the outer oxide, indicated the existence of Ti_2O, ε-TiN and TiN phases in addition to TiO_2 for all samples pretreated with nitrogen and subsequently reacted in either oxygen or air, or oxidized in only air. No X-ray patterns were taken from the alloy exposed to only pure nitrogen. Tables V and VI illustrate the type of the numerous X-ray data obtained from most of the samples exposed to various environments at different temperatures.

To investigate the relative depth of the nitride phases and their orientation some samples were polished to various depths, after prior removal of the outer scale, and X-ray diffractometer scans were made at each of the depths into the samples. Table VII illustrates the data obtained for the case of prenitridation of the alloy for 12 hr at 980°C followed by oxidation in oxygen at the same temperature for additional 12 hr. The TiN lines disappeared after the first polish thus indicating that this phase constitutes a rather thin layer of the inner scale. The ε-TiN and Ti_2O lines disappeared with the second polish and a very intense line at $\theta = 62.95°$ appeared. It was identified as a line from the (110) plane, which corresponds to the $(11\bar{2}0)$ planes in the hcp system of α-Ti. Further polishing into the sample brings out other α-Ti lines. The table contains also data from the alloy before exposure to nitrogen. Similar results were obtained for samples oxidized in air after nitridation.

From the present X-ray investigations, the nitrides seem to be highly oriented to planes with "d" spacings of about 1.5 Å. The TiN phase is oriented to the (220) planes with $d \simeq 1.496$ Å, whereas the ε-TiN phase is oriented to the (113) planes with $d \simeq 1.514$ Å. Similarly, the α-Ti phase seems to be oriented to the (110) planes having $d \simeq 1.475$ Å.

It should be noted that all X-ray diffractions were obtained on samples at room temperature.

Table V. X-Ray Diffractometer Data from Outer and Inner Oxide Scales Formed on Ti–4.32 wt.%Nb Alloy Oxidized in Oxygen (12 hr) at 1123°C After Nitridation (12 hr) at 1123°C[a]

	Outer oxide surface,	Inner scale surface			
d(exp)	TiO_2	TiO_2	Ti_2O	ε-TiN	TiN
3.450 m	—	—	—	3.490	—
3.250 s	3.245	3.245	—	—	—
2.560 vw	—	—	2.563	—	—
2.490 w	2.489	2.489	—	—	—
—	—	—	—	2.460	—
2.440 vw	—	—	—	—	2.440
2.384 vw	—	—	2.422	—	—
2.300 w	2.297	2.297	—	—	—
2.274 s	—	—	—	2.282	—
(2.268 m)	—	—	2.265	—	—
2.200 m	—	—	—	2.205	—
2.190 w	2.118	2.118	—	—	—
2.102 w	—	—	—	—	2.120
1.932 w	2.054	2.054	—	—	—
1.779 w	—	—	—	1.784	—
1.750 vs	—	—	1.761	—	—
—	1.687	1.687	—	—	—
1.620 w	1.624	1.624	—	—	—
—	—	—	1.615	—	—
1.527 w	—	—	—	1.514	—
1.500 s	—	—	—	—	1.496
1.487 m	1.480	1.480	1.480	—	—
1.458 m	1.453	1.453	—	—	—
1.449 vw	—	—	—	1.448	—
—	—	—	—	1.338	—
—	—	—	—	1.369	—
1.365 vw	—	—	1.366	—	—
(1.355 m)	1.360	1.360	—	—	—
1.350 vw	1.347	1.347	—	—	—

[a]Cu radiation, 30 kV, 15 mA. d is planar spacing in Å. Intensity of lines (I/I_0): vs = very strong, s = strong, m = medium, w = weak, vw = very weak.

Electron Microprobe Analysis

Electron microprobe scans for concentration profiles of T, Nb, O, and N in the metal taken through cross sections of some of the nitrogen pretreated samples of Ti–4.32 wt.% Nb alloy are shown in Figs. 9–11. The original intensity data were converted to concentrations by a computerized program with appropriate corrections for background intensity, X-ray fluorescence, atomic number differences, and absorption of X rays from one element by another. The occurrence of a peak in the oxygen concentration profile, in all

Table VI. Debye–Scherrer X-Ray Patterns from Outer Oxide Scale Formed on Ti–4.32 wt.%Nb Alloy Oxidized in Either Oxygen (12 hr) at 895°C After Nitridation (12 hr) at 896°C or in Air (12 hr) at 985°C After Prior Nitridation (12 hr) at 983°C[a]

d(file)[b], Å	(hkl)	O_2 after N_2 d(exp), Å	Air after N_2 d(exp.), Å
3.245	110	3.210 vs	3.231 vs
2.489	101	2.480 s	2.477 s
2.297	200	2.291 m	2.288 m
2.188	111	2.180 s	2.184 s
2.054	210	2.048 m	2.052 m
1.687	211	1.679 vs	1.684 vs
1.624	220	1.621 s	1.622 s
1.480	002	1.474 m	1.475 m
1.453	310	1.450 m	1.452 m
1.360	301	1.360 s	1.360 s
1.347	112	1.345 m	1.352 m
1.305	311	—	—
1.243	202	1.239 vw	1.242 vw
1.200	212	—	—
1.170	321	1.169 w	1.169 w
1.1485	400	1.148 w	1.146 vw
1.1329	410	—	—
1.0932	222	1.092 m	1.091 vw

[a] The only phase present is TiO_2–rutile. Cu radiation, Ni filter, 30 kV, 15 mA, 12-hr exposure; abbreviations as in Table V.
[b] X-ray Powder Diffraction File, published by ASTM, Philadelphia, Pennsylvania.

of the examined samples, is of some interest. At the temperatures of the gas–metal reactions, the alloy is in the bcc β-Ti crystallographic form which upon oxidation or nitridation transforms to hcp α-Ti structure while the inner core of the specimen remains still in the β-Ti form, for the reaction times involved (12 hr total), and this phase, in turn, transforms by a martensitic reaction to α'-Ti during cooling of the specimen to room temperature. It is suggested that the oxygen peak occurs at the α-Ti/α'-Ti interface. Metallographic examinations of the polished cross sections seem to confirm the location of the peak at this interface. From these examinations it can also be concluded that the oscillations in the Nb concentration profile coincide with the grain boundaries. It should be noted that the nitrogen profile drops continuously off to zero at a relatively short distance into the metal substrate, except for samples subjected only to nitridation (Fig. 11) where it behaves similarly to the oxygen profile.

Table VII. X-Ray Diffractometer Results from Various Depths of the Inner Scale of the Ti–4.32 wt.%Nb Alloy Which Was Oxidized at 980°C for 12 hr After Prior Nitridation for the Same Time and at the Same Temperature[a,b]

						Polished			
2θ; deg	d; Å	Identification		Before exposure	Inner scale	#1	#32	#3	Center
35.05	2.557	(010)	α-Ti	(+0.005) w	—	—	(−0.02) w	(−0.02) vs	(−0.02) w
38.40	2.342	(002)	α-Ti	(+0.018) s	—	—	—	—	—
39.45	2.282	(102)	ε-TiN	—	(−0.008) m	(−0.004) m	(−0.002) s)	—	—
39.75	2.265	(101)	Ti_2O	—	(+0.003) vs	(−0.002) vs	—	—	—
40.15	2.244	(011)	αTi	(+0.019) vs	—	—	(−0.01) w	(−0.01) w	(−0.008) w
42.60	2.120	(200)	TiN	—	(−0.013) s	(+0.015) m	—	—	—
51.15	1.784	(202)	ε-TiN	—	(−0.03) m	—	—	—	—
50.90	1.761	(102)	Ti_2O	—	(−0.016) m	(−0.01) m	—	—	—
53.00	1.726	(012)	α-Ti	(+0.006) m	—	—	—	(+0.006) w	—
59.90	1.514	(113)	ε-TiN	—	(−0.025) vs	(−0.02) s	(−0.02) w	—	—
62.00	1.496	(220)	TiN	—	(−0.007) m	(−0.007) w	—	—	—
62.70	1.480	(110)	Ti_2O	—	(+0.005) s	(−0.002) w	—	—	—
62.95	1.475	(110)	α-Ti	(+0.008) w	—	—	(−0.001) w	(−0.001) s	(−0.001) vs
64.25	1.448	(222)	ε-TiN	—	(+0.004) w	—	—	—	—
70.65	1.332	(103)	α-Ti	(+0.004) m	—	—	(−0.012) w	(−0.012) m	(−0.012) vs

[a] Cu radiation, 30 kV, 20 mA; abbreviations as in Table V.

[b] Legend: d spacings and Bragg angle were obtained from ASTM X-ray file. Plus or minus sign indicates difference in obtained d data from file data. #1, #2, #3 indicate increasing depth from the inner scale into the sample.

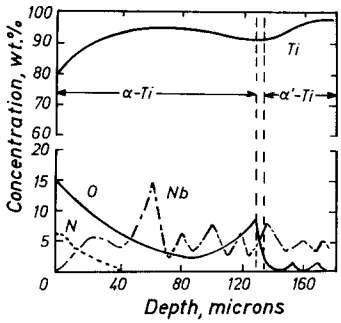

Fig. 9. Electron microprobe analysis of the metal substrate of Ti–4.32 wt.%Nb alloy pretreated in nitrogen for 12 hr at 980°C and next oxidized in oxygen for 12 hr at 980°C. Data taken in 4-μ steps.

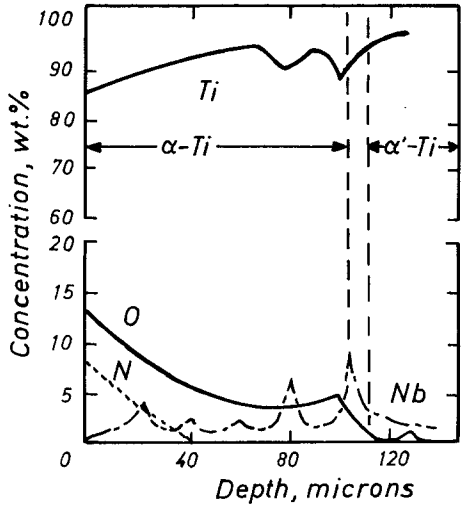

Fig. 10. Electron microprobe analysis of the metal substrate of Ti–4.32 wt.%Nb alloy pretreated in nitrogen for 12 hr at 986°C and next oxidized in air for 12 hr at 999°C. Data taken in 4-μ steps.

Microhardness

Vickers microhardness measurements taken across the thickness of the gas-reacted Ti–4.32 wt.%Nb alloy specimens are shown in Fig. 12. The data were obtained by utilizing a 30-g load and the objective-filar reading corresponds to about ±30 DPN at DPN values around 600. The dashed horizontal line indicates the hardness before subjecting the material to nitrogen pretreatment. It should be noticed that the hardness gradients are consistent with the microprobe data (Figs. 9–11) for oxygen, and that oxygen

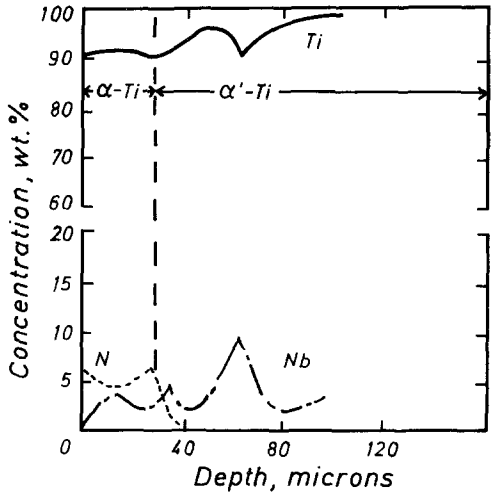

Fig. 11. Electron microprobe analysis of the metal substrate of Ti–4.32 wt.%Nb alloy after nitridation for 12 hr at 999°C. Data taken in 4-μ steps.

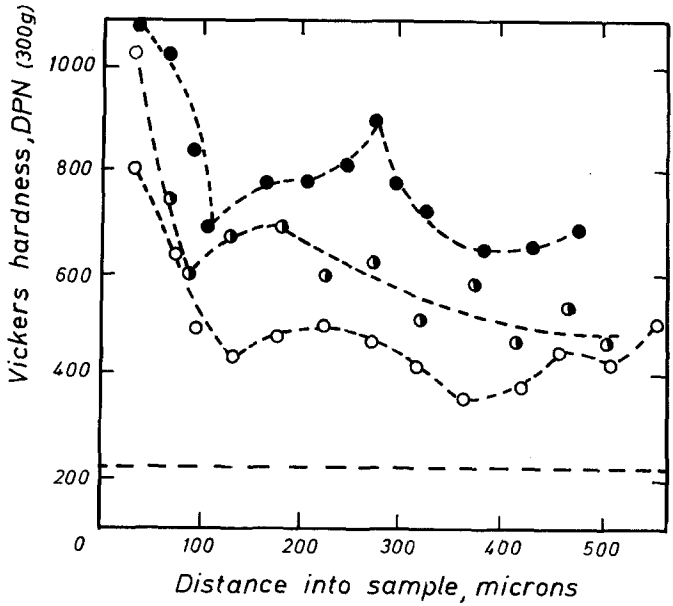

Fig. 12. Vickers hardness of metal substrate of gas reacted Ti–4.32 wt.%Nb alloy. (○) after nitridation at 999°C for 12 hr. (◑) after nitrogen pretreatment at 986°C for 12 hr and oxidation in air at 999°C for 12 hr. (●) after nitrogen pretreatment at 980°C for 12 hr and oxidation in oxygen at 980°C for 12 hr.

penetrated throughout the entire sample thickness or else some other mechanism of hardening of the metal core occurred.

DISCUSSION

The fact[2] that oxidation of Ti–4.32 wt.%Nb alloy in air, in the temperature range 900–1000°C, occurs at a considerably slower rate than in oxygen has prompted the present investigation on the effect of nitrogen pretreatment on the subsequent oxidation kinetics of the alloy. In general, nitrogen pretreatment followed by oxidation in pure oxygen resulted in reaction rates comparable to those in air alone (see Table II). Prenitridation reduces, however, the reaction rates of subsequent oxidation of the alloy in air at all of the investigated temperatures; the largest reduction being about 26% at 999°C. Similarly, at any temperature, oxidation after nitridation is lower than oxidation for the same period of time in only oxygen. Thus, e.g., at 895°C the alloy oxidizes 17 times faster than it does in nitrogen pretreated condition.

The obtained activation energy of 50.31 kcal/mole for the initial parabolic rates in pure oxygen is in close agreement with 51 kcal/mole reported[8] for pure Ti. Nitrogen pretreatment before oxidation in oxygen decreases the activation energy from 50.31 to 37.60 kcal/mole, whereas such a pretreatment has little effect on the activation energy for subsequent oxidation in air (see Table III). The measured nitridation rates (see Table I) of the Ti–4.32 wt.%Nb alloy are comparable to those reported by Gulbransen and Andrew[5] for pure Ti, if their results are extrapolated above the upper temperature of 850°C used by the authors.

The existence of the nitride layers of the fcc δ-TiN, which is commonly reported in the literature as TiN, and of the tetragonal ε-TiN as evidenced by X-ray analysis (see Tables V and VII) seems to hinder oxidation of the metal substrate by acting as a protective barrier for oxygen diffusion. It is likely that the titanium nitrides, being thermodynamically less stable[9] in the temperature range of the present investigation than titanium oxides,[10] decompose in the presence of oxygen to form TiO_2 or Ti_2O and gaseous nitrogen. That such a reaction is feasible, the work of McQuillan and McQuillan[11] can be cited to show that at high temperatures TiN dissociates to form TiO_2 (rutile) when exposed to oxygen. Part of the nitrogen thus liberated at the TiO_2–TiN interface diffuses inward across the (TiN+Ti_2O) layer and reacts with ε-TiN to form TiN. Also some of the oxygen that has diffused through the TiN layer reacts with ε-TiN to form Ti_2O and gaseous nitrogen. Some of the unused oxygen and nitrogen diffuse further across the ε-TiN to react with α-Ti to form more Ti_2O and ε-TiN. The remainder of the oxygen and nitrogen diffuses into the α and then β solid solutions of

Ti + 4.32 wt.% Nb. Of course, some of the nitrogen formed at the TiO_2–TiN interface may diffuse outward across the oxide. It is suggested that the inward diffusion of nitrogen is dominant. Should the reverse be true then the nitride layers would vanish. The oxidation model just formulated applies to oxidation in oxygen of the prenitrided alloy and for the case of oxidation in air after nitridation the same model should hold true, except that additional nitrogen from air diffuses across the appropriate layers of the scale and no outward nitrogen flux is expected. Fig. 13 is a schematic representation of the proposed model. It also includes the suggested boundary reactions.

It should be noted that ε-Ti_3N (or ε-Ti_4N) and Ti_2O are here considered as gas-saturated phases of the α-(Ti + 4.32Nb) solid solution. Supporting evidence for this is provided by gas contents in the surface at the metal/inner-scale interface. From Figs. 9 and 10 the average oxygen content is about 14 wt.%, which corresponds to the saturation solubility[12] of 13.7 wt.% O in pure α-Ti at 1000°C. Similarly Figs. 9, 10, and 11 give about 6.5–8 wt.% N and the saturation solubility[6] of N in pure α-Ti is 7.1 wt.%. The present experimental values for oxygen content yield a ratio of O/Ti = 0.505 or a composition of $Ti_{1.98}O$. Identical calculation based on the electron microprobe analysis of the average nitrogen content of 7.25 wt.% give a ratio of N/Ti = 0.300 which corresponds to $Ti_{3.33}N$ for Figs. 9 and 10 and a ratio of N/Ti = 0.247, i.e., $Ti_{4.05}N$, for Fig. 11; the average formula being $Ti_{3.69}N$. Although this composition in different than ε-Ti_2N reported by McDonald and Wallwork,[6] it is, however, in close agreement with Ti_3N or Ti_4N both of which are reported by Palty *et al.*[13] The present electron microprobe data thus corroborate our assumption that the oxygen and/or nitrogen saturated α-(Ti+4.32Nb) solid solutions can be expressed by Ti_2O and ε-Ti_3N formulas. No explanation can be given at this time for the

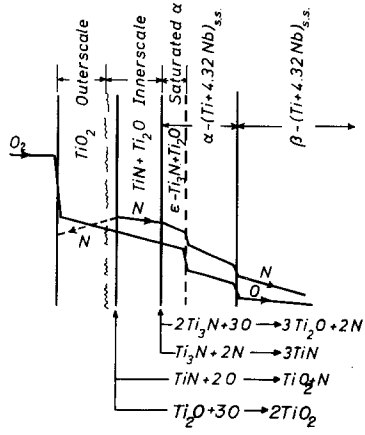

Fig. 13. Schematic presentation of oxidation model of prenitrided Ti–4.32 wt.% Nb alloy at temperature above the α/β-Ti transformation and at oxidation time $t > 0$.

observed increase in oxygen and nitrogen contents at the α-Ti/α'-Ti interface.

Since hardness measurements (see Fig. 12) depend on both nitrogen and oxygen concentrations in the metal our data are not conclusive but they indicate, at least quantitatively, that the Vickers hardness drops from the surface into the sample and follows the oxygen profiles as determined by the electron microprobe analysis.

The oxide sintering experiments, that is, oxidation of the alloy either in air or oxygen at a temperature 100°C higher than the temperature of the initial and final oxidation periods, were not successful in reducing the reaction rates with the exception at 1200°C where the k_p value for the last 4-hr period is somewhat lower than for the presintering period (see Table IV). Since no measurements of scale thickness have concurrently been made with the kinetic measurements the reasons for the failure are not obvious. One possible explanation can be that the sintering period of 4-hr duration was not long enough to yield a compact and well-recrystallized scale.

ACKNOWLEDGMENTS

The financial support of the Naval Air Systems Command, Department of U.S. Navy, Washington, D.C., under the contract No. N62269-73-C-0520 is gratefully acknowledged. Assistance of Mrs. M. Langer and Mrs. D. Kupfermann in typing and drafting, respectively, is appreciated.

REFERENCES

1. H. W. Maynor, B. R. Barrett, and R. E. Swift, WADC Tech. Rep. 54-109, Contract No. AF 18 (600)-60, March 1955.
2. C. J. Rosa, Final Report from University of Cincinnati to Naval Air System Command, Department of U.S. Navy, Contract No. N 62269-72-C-0520, January 1974.
3. K. Hauffe, *Oxidation of Metals* (Plenum, New York, 1965) p. 14 ff., p. 221.
4. L. G. Carpenter and F. R. Reavell, *Metallurgia* **39**, 63 (1949).
5. E. F. Gulbransen and K. F. Andrew, *Metall. Trans.* **185**, 741 (1949).
6. N. R. McDonald and G. R. Wallwork, *Oxid Met.* **2**, 263 (1970).
7. A. Münster and G. Schlamp, *Z. Phys. Chem. (Leipzig)* **13**, 76 (1957).
8. P. Kofstad, P. B. Anderson, and O. J. Krudtaa, *J. Less-Common Met.* **3**, 89 (1961).
9. P. Grieveson, *Proc. Br. Ceram. Soc.* **8**, 137 (1967).
10. F. D. Richardson and J. H. E. Jeffes, *J. Iron Steel Inst. London* **160**, 261 (1948).
11. A. D. McQuillan and M.. K. McQuillan, *Titanium* (Butterworths Scientific Publications, London, 1956) pp. 307–333.
12. T. H. Schofield and A. E. Bacon, *J. Inst. Met.* **84**, 47 (1955/56).
13. A. E. Palty, H. Margolin, and J. P. Nielsen, *Trans. Am. Soc. Met.* **46**, 312 (1954).